Afyon Kocatepe Üniversitesi Fen ve Mühendislik Bilimleri Dergisi
Afyon Kocatepe University – Journal of Science and Engineering
https://dergipark.org.tr/tr/pub/akufemubid

Araştırma Makalesi / Research Article
DOI: https://doi.org/ 10.35414/akufemubid.1467210
AKÜ FEMÜBİD **24** (2024) 067202 (1506-1515)
AKU J. Sci. Eng. **24** (2024) 067202 (1506-1515)

The Evaluation of Mechanical Properties of Commercial Composite Bones and 3D-Printed Bones Produced Using the CJP Technology

Makale Bilgisi / Article Info
Alındı/Received: 09.04.2024
Kabul/Accepted: 05.08.2024
Yayımlandı/Published: xx.xx.xxxx

Ticari Kompozit Kemiklerin ve CJP Teknolojisi Kullanılarak Üretilen 3B Baskılı Kemiklerin Mekanik Özelliklerinin Değerlendirilmesi

Samet ÇIKLAÇANDIR*, Yalçın İŞLER

İzmir Katip Çelebi University, Engineering and Architecture Faculty, Department of Biomedical Engineering, İzmir, Türkiye

Abstract

Cadaver bones and artificial bones are utilized to perform preoperative studies and education purposes. Cadaver bones are hard to find, require ethical permissions, and have infection hazards. Therefore, commercial artificial bones are preferred in practice. Nonetheless, since these commercial alternatives are standardly produced in an average size and geometry, it is almost impossible to adapt them to a specific surgical simulation. In addition, these artificial bones have relatively high costs, which limits their accessibility. On the other hand, ColorJet printing (CJP), one of the three-dimensional printing technologies, offers a rapid and cost-effective alternative. However, whether the printed 3D-printed models can mechanically comply with artificial bones is unclear. In this study, 3D-printed bones and artificial commercial composite bones were compared in terms of mechanical properties. Compression tests were applied over 14 printed and 14 composite bones using the ISO 5833 standard. Mechanical properties including stress-strain, load to failure, and elastic modulus were calculated, and these results were compared using the two-sample independent t-test, which is one of the statistical analysis methods. Consequently, there was no significant difference between the bone models in terms of stress and failure load values ($p<0.52$ and $p<0.17$, respectively), however, the elastic modulus was statistically significant ($p<0.01$). These test findings demonstrated that this technology, which has a faster production capacity than other methods, can show similar strength to artificial bones. Thus, 3D-printed bones can be utilized instead of artificial bones in preoperative planning, which needs patient-specific bone models, and experimental biomechanical studies.

Keywords: *Additive manufacturing; Commercial composite bones; Preoperative applications; CJP technology; Three-dimensional printing.*

Öz

Kadavra kemikleri ve yapay kemikler, ameliyat öncesi çalışmalar gerçekleştirmek için ve eğitim amacıyla faydalanılmaktadır. Kadavra kemiklerini bulmak zordur, etik izinler gerektirir ve enfeksiyon tehlikesi barındırırlar. Bu yüzden uygulamada ticari yapay kemikler tercih edilmektedir. Bununla birlikte, bu ticari alternatif standart olarak ortalama bir boyut ve geometride üretildiğinden onları belirli bir cerrahi simülasyona uyarlamak neredeyse imkansızdır. Ayrıca, bu yapay kemikler, erişilebilirliklerini sınırlayan nispeten yüksek maliyetlere sahiptir. Diğer yandan, üç boyutlu (3B) baskı teknolojilerinden birisi olan ColorJet baskı (CJP) hızlı ve uygun maliyetli bir alternatif sunmaktadır. Fakat 3B'lu baskılı modellerin mekanik olarak yapay kemiklere uyum sağlayıp sağlayamayacağı belirsizdir. Bu çalışmada, 3B'lu baskılı kemikler ile yapay ticari kompozit kemiklerin mekanik özellikler açısından karşılaştırması gerçekleştirilmiştir. ISO5833 standardı temel alınarak basma testleri 14 baskılı ve 14 kompozit kemiklere uygulanmıştır. Gerilme-şekil değiştirme, kırılma yükü ve elastik modülü gibi mekanik özellikler hesaplanmış ve bu sonuçlar istatistik analiz yöntemlerinden birisi olan iki örnekli bağımsız t-testi kullanılarak karşılaştırılmıştır. Sonuç olarak, kemik modelleri arasında gerilme ve kırılma yük değerleri açısından anlamlı bir fark bulunmamıştır (sırasıyla $p<0.52$ ve $p<0.17$), ancak elastik modülü istatistiksel olarak anlamlıdır ($p<0.01$). Bu test sonuçları, diğer yöntemlere göre daha hızlı üretim kapasitesi bulunan bu teknolojinin yapay kemiklerle benzer dayanıklılık gösterebileceği ortaya çıkarılmıştır. Böylece hastaya özel kemik modelleri gerektiren ameliyat öncesi planlamada ve deneysel biyomekanik çalışmalarda yapay kemikler yerine 3B baskılı kemikler kullanılabilir.

Anahtar Kelimeler: *Katmanlı üretim; Ticari kompozit kemikler; Ameliyat öncesi uygulamalar; CJP teknolojisi; Üç boyutlu baskı.*

1. Introduction

Artificial bones are frequently used in health science education, preoperative planning, biomechanical studies, and finite element analysis-based validation process (Nagl 2021). They are produced from Polyurethane (PU) foams consisting of bone-mimicking material (Navarro *et al.* 2008). There are four generations in the production technology. The first-generation artificial bones consisted of basic materials such as plastic and simple metal, which were easily shaped and had low cost. The second generation consisted of synthetic materials such as epoxy resin and PU foam, enabling more realistic surgical practices than the previous one. The bones from the first and second generations have very low strength values compared to real bones and not being able to imitate

*Sorumlu Yazar/Corresponding Author: Samet ÇIKLAÇANDIR e-posta/e-mail: samet.cikla@gmail.com

natural bone well (Victor and Muthu 2014). The third generation includes composite materials made up of varied polymers that outperform the previous ones in mimicking bone's cortical and cancellous structures. The fourth generation contains composite materials that are more reinforced compared to the third and provided results that were mechanically close to natural bone. Bones from the third and fourth generations have closer strength and stiffness values to the real bones (Elfar *et al.* 2014). These new-generation bones are good alternatives to real bones to use in academic studies and education. These models have similar mechanical, thermal, and drilling properties to the real bone (Gardner *et al.* 2010). On the other hand, thanks to advanced technology, artificial bones not only provide mechanical properties but also the future generation artificial bones, called bioinspired materials, which play a biologically active role and can be customized such as the three-dimensional printing (3DP), are beginning to take their place today.

Artificial bones are preferred in many studies since their use does not require ethical permission (Hausmann 2006). In addition, they have a standardized shape, which increases the reproducibility, so that the achieved results can easily be compared to the literature. The use of artificial bones also prevents possible infection risks and does not require special storage techniques. In addition to all of these advantages, artificial bones also allow performing a bone-based study in a limited time. On the other hand, there are some drawbacks in using artificial bones. Artificial bones cannot mimic real bones from cadavers perfectly. In addition, new-generation bones are quite expensive, and it becomes a challenge in low-budget academic and educational studies, especially. Since their product is standard in shape, to conduct an academic study that requires different bone sizes is impossible by using artificial bones only. To overcome these drawbacks, three-dimensional printing technology may be a low-cost alternative since it represents promising rapid developments in its mimic ability (Lim *et al.* 2016), recently.

3DP technologies can be categorized as Fused Deposition Modeling (FDM), Selective Laser Sintering (SLS), Stereolithography (SLA), powder-based or ink-jet, Direct Metal Laser Sintering (DMLS), Selective Laser Melting (SLM), and Digital Light Processing (DLP) (Cheng *et al.* 2021). The first four technologies, however, are the most widespread and considered fundamental. In the FDM method, thermoplastic materials are melted using a hot nozzle, and a product is formed via nozzle movements. This technology has found common use due to its easy-to-use structure, its affordable material prices, and its low initial cost (Dudek 2013). Also, produced parts exhibit remarkable resistance to different physical abrasives throughout time. However, the use of supports in this technique limits the mimic ability and surface finishing (Kudelski *et al.* 2017). In addition, properly controlling the melting temperatures of thermoplastic materials can be highly challenging to achieve the required fluidity and adhesion. The SLS technology produces parts through sinter-powered materials such as plastic, metal, or ceramic powders using a laser (Fina *et al.* 2017). Printers manufactured as SLS are very costly and have problems occupying large areas, and complex printing processes (Wu *et al.* 2008). The SLA technology produces models by solidifying the resin liquid using UV light. It allows printing parts with very fast, low-cost, and high-resolution (Shahrubudin *et al.* 2019). However, it is not very common in biomechanical studies due to the need for support, the fragility of parts, and the inability to mimic bone tissue (Miedzinska *et al.* 2020). In addition to these technologies, the Binder Jetting (BJ) method prints parts by combining powders with a binder and it can manufacture artificial bones of similar size and porosity to real bones (Zhang *et al.* 2021). ColorJet Printing (CJP) uses the BJ technology and it can print parts in colour without needing support (Kim *et al.* 2016). Due to these properties, it can produce useful bone models in biomechanical and anatomical studies (Bakhtiar *et al.* 2018). A brief comparison of these technologies is given in Table 1.

Table 1. Comparison of the most common 3D printer Technologies

3D Printer Tech.	Pros	Cons
FDM	Simple prototyping Lowest price Time-resistant parts	Low details Limited designs Difficulty in temperature control
SLS	High resolution No support structures Multiple productions	Rough surface Long drying time Expensive 3D machines
SLA	Highest resolution Low material consumption Fast prototyping	Fragile resin parts Sensitive to sunlight Need for support structures
CJP	High resolution No support structures Fast prototyping	Long drying time Difficulty of use Binder requirement

CJP technology coagulates calcium sulfate-based powders, which cover the printer bed, using a binder (Brunello *et al.* 2016). The binder is sent from the feeder to the movable print-head. After the binder is injected into the powder parts, the build piston moves down one layer and is filled from the powder supply through a

leveling roller (Awari *et al.* 2021). When the printing is complete, a particular period is waited for the printout to dry, and the unbound powder particles on it are removed with the help of a blower to be recycled. The part can be immersed in a binder-filled container to increase strength (Ziaee and Crane 2019). Color printouts can be performed with the CJP method, and vessels, ligaments, and muscles can be distinguished in different colors (Lee *et al.* 2017). Therefore, anatomical models can be produced using CJP technologies in accordance with biofidelity and can be utilized in training, preoperative planning, and biomechanical tests (Al-Dulimi *et al.* 2020).

3D printing has proven its advantages over medical education, and preoperative planning (Mihcin and Ciklacandir 2022). Among them, preoperative planning aims to investigate all possible situations before the operation starts, which increases the success ratio of operations drastically (O'Toole III *et al.* 1995).

On the other hand, bones are composed of porous structures, this requires intricate 3D technologies (Du *et al.* 2020). The validation studies showed that the printed bones have similar mechanical and material properties to the real bones (Lv *et al.* 2019). For example, Tai et al. compared 3D-printed bone models with synthetic bones in thermal and mechanical properties (Tai *et al.* 2018). They showed that the thermal and drilling properties of 3D models were similar to those of cortical bones. Xu et al. used a 3D-printed artificial bone, which is printed with an FDM printer using a processed CT scan image, to repair a goat femur (Xu *et al.* 2014). In another study, Hochman et al. showed that real sheep bones and 3D printed artificial bones, which are produced with BJ technologies, have similar mechanical properties (Hochman *et al.* 2014).

In a general preoperative study, the core idea is to manufacture a prototype of the body part using a 3D printer, and then the operator simulates the surgery. For this purpose, the Digital Imaging and Communications in Medicine (DICOM) file of the patient is obtained from computer tomography (CT) or magnetic resonance imaging (MRI) methods first. These images are segmented and processed by dedicated computer programs and exported as STL files (Cimerman and Kristan 2007). Next, these files are converted to G-Code, which is the language of 3D printers, and transferred to the 3D printer (Blaszczyk *et al.* 2021). Figure 1 shows the right and left femoral heads, which were reconstructed to adhere strictly to the DICOM file obtained from a patient and printed with CJP technology in our laboratory (Mihcin and Ciklacandir 2022).

Figure 1. Right and left femoral head specimens printed with ColorJet Printing (CJP) technology

Since CJP technology has numerous advantages including low-cost solution, high resolution, and rapid prototyping, it can be considered to use in preoperative biomechanical studies. Although this technology is proven in animal studies, there is no comparison to real human bones or commercially manufactured bone models. In this study, we aimed to compare the mechanical properties of 3D-printed tibial sawbones to those of artificially produced commercial composite bones.

2. Materials and Methods

2.1 Material preparation

A total of 14 composite tibial Sawbones® manufactured from glass-reinforced epoxy material (Third-Generation, Pacific Research Laboratories, Vashon, WA) was prepared for mechanical tests. Because of how closely their mechanical characteristics and geometry resembled those of natural bones, these artificial bones were chosen. In accordance with ISO 5833 guidelines, the specimens were sliced into cylindrical shapes with a 25 mm radius and a 10 mm height. Specimens were detached at the middle of the bone shaft so that experiments provided consistent results. This point was preferred because the material properties of the specimen were more homogeneously distributed, easy to sample and standardize, and reproducibility of experiments. In some specimens, a perfect cylindrical geometry could not be achieved as in 3D printing specimens. To prevent this from affecting the results, the surface area was calculated by taking images of each specimen via the surface area calculator.

Cylindrical specimens were created with the same dimensions in SolidWorks (v.2016, SolidWorks Corp., MA, USA) and transferred to 3DPrint™ (v1.0, 3D Systems, Rock Hill, South Carolina) software in the STL file format (Figure 2). Using ColorJet Printing (CJP) technology, they were manufactured using the Projet 160 3D printer (3D Systems, Rock Hill, SC, USA). In the CJP technique, the

layer thickness was adjusted at 0.1 mm, which is regarded as a relatively high value of 0.17 mm in the FDM method. Following the completion of the printing process, the powder particles (VisiJet® PXL™ Core) were bonded with a binder (PXL™ Binder) and dried for about two hours.

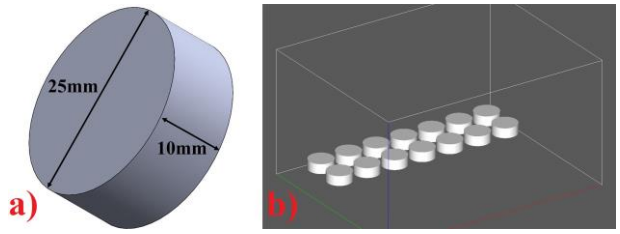

Figure 2. a) Specimen dimensions for ISO 5833 standards, b) Placement of specimens in the building area

2.2 Mechanical test

The compression test is a method based on the principle of shortening or pressing the length of a specimen by applying a compressive load to the material (Beaupied *et al.* 2007). Using the Shimadzu AG-IC tester (Shimadzu Corp., Kyoto, Japan), the specimens were subjected to the compression test. The load cell has a 10kN capacity, which is more than sufficient, and throughout the experiment, the test speed is set at 1mm/m. A compressive test was applied with a maximum displacement of 3 mm for each specimen. Since this is considered to be the greatest displacement at which the specimens could fail. Figure 3a illustrates the implementation of a compression test on composite bones. Similarly, a printed bone specimen in the experiment and its failure status after the test are shown in Figure 3b-c. The results of the analysis recorded by Trapezium X software during tests were used to derive the values of compressive stress, strain, and elastic modulus. The following section provides a brief explanation of the formulae used to compute all of this.

Stress is the amount of force acting on a unit area. In compression or axial loading, a force is applied perpendicular to the surface area to deform the material. After escalating force magnitude gradually on a specimen, the failure point, which occurs at any time, is the place at which deformation starts and becomes an irreversible process for the material. Stress is calculated with

$$\sigma\ (MPa) = \frac{F\ (N)}{A\ (mm^2)} \qquad (1)$$

where *F* represents the applied force, *A* is the cross-section area, and σ is the stress.

Strain refers to how much material under load changes its shape compared to the state before the load is applied. The calculation of strain is represented by the following formula

$$\varepsilon = \frac{\Delta L\ (mm)}{L_0\ (mm)} \qquad (2)$$

where ε denotes the strain, ΔL is the total elongation, L_0 is the original length. A stress-strain diagram is the most common way to analyze the material's relationship between stress and strain. By computing the slope in the elastic region of this graph, characteristic information unique to each material can be gathered. Among these, the elastic modulus is the most frequently encountered expression. It states the deformation property of a material to return to its original shape under low stresses after this stress is removed. The stress and strain are directly proportional in the elastic region (Hooke's law) as

$$E\ (MPa) = \frac{\sigma\ (MPa)}{\varepsilon} \qquad (3)$$

where *E* is elastic modulus.

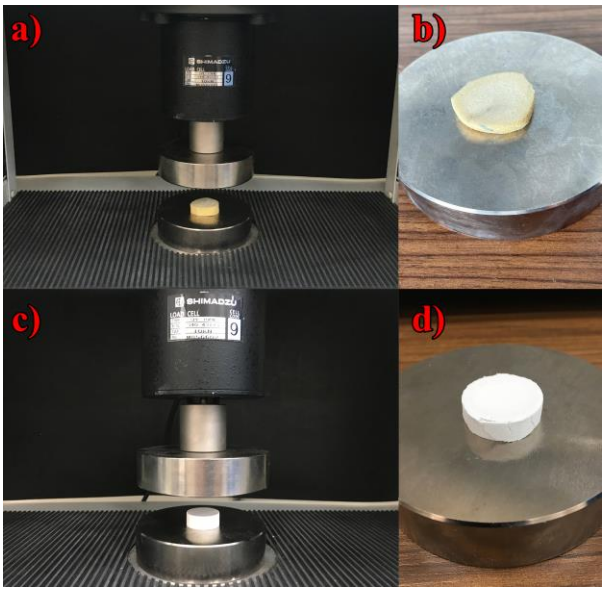

Figure 3. Before and after compression test of specimens (a-b) Composite tibial Sawbones (c-d) Printed specimens, respectively

2.3 Statistical analysis

Statistical analysis was performed to determine the difference between the groups whose calculations were completed as mentioned in the previous section. To ascertain whether or not there was a statistically significant difference between the two groups, the independent t-test (sometimes called a two-sample t-test) was employed. The computation of this test involves dividing the difference between the two sample means by the estimated standard error, which can be either pooled or unpooled. All analysis of specimens was computed on the SPSS (v.25, IBM, NY, USA) software. If a test result is less than 0.05 level, then it can be concluded that there is a significant difference between these two groups for the corresponding parameter.

3. Results

The total printing time of the parts produced with 3DP took 32 minutes. It was used a 21.2 ml binder for cylinders printed in monochrome. The total volume of parts was obtained at 68.6 cm^3, and the total surface area was calculated at 247.1 cm^2. The printing information estimated by printer software about a specimen is necessary to calculate the cost of the material. Consequently, the estimated cost of printing needed to produce 3DP bone that resembles composite bone is $15 per bone.

Results of composite bone and printed bone specimens are graphed in Figures 4a–b in the force versus displacement. In the first figure, composite bone specimens had slightly different results, the reason is that they were collected at different times and the effect of waiting periods. With composite bone specimens, a force-driven horizontal movement appeared at a displacement of approximately 3 mm and maximum force values were obtained for all. Accordingly, the maximum failure loads were observed at 4707.5 N for composite bones and 4565.6 N for 3DP cylinders. In addition, it emerged that while results differed amongst themselves for composite bone, 3D-printed specimens showed very consistent results. Stress and strain results derived from the force/displacement graphs are given in Figures 4c-d. These graphs, which are required to determine the elastic modulus, resemble the force/displacement graph quite a bit. In 3DP specimens, the highest stress was recorded at 8.97 MPa, whereas it was obtained at 11.71 MPa in composite bones. The visualization of only five specimen results is shown in Figure 4b-d due to the high degree of similarity among the 3D-printed specimens.

For both groups, the elastic modulus values computed using equation (3) are given in Table 2. The maximum elastic modulus value of composite bones was 71.51 MPa, while the lowest value was 15.60 MPa. On the other hand, the maximum elastic modulus of the 3DP models was 191.59 MPa, and the minimum elastic modulus was 120.77 MPa. Comparing 3D-printed specimens to composite bone, higher means were observed for stress, strain, and elastic modulus. During the experiment, failure points were also observed and the results for both groups are given in the same table.

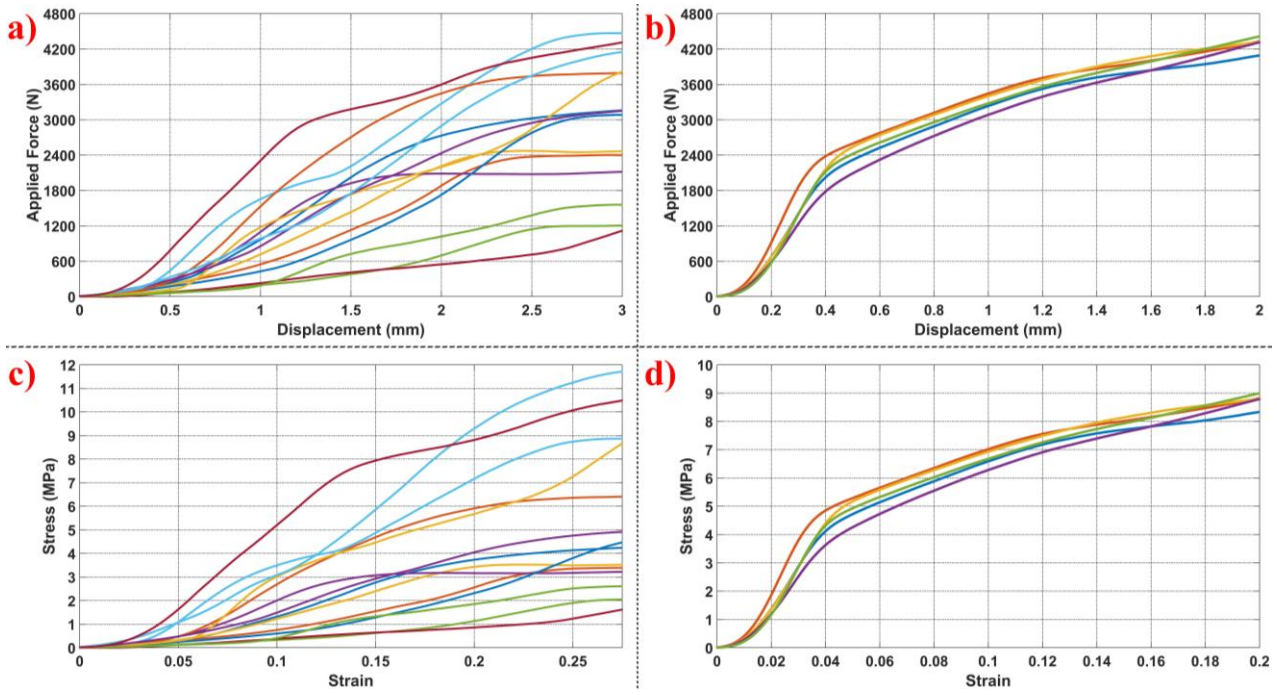

Figure 4. Compression test results (a) Force-Displacement graphs of composite bones (b) Force-Displacement graphs of 3DP cylinders (c) Stress-Strain graphs of composite bones (d) Stress-Strain graphs of 3DP cylinders.

Table 2. Mechanical comparison of 3DP cylinders with composite bones

	Units	Number of Samples (N)	Composite Bones (Mean ± SD)	3D-Printed Cylinders (Mean ± SD)	p
Compressive Stress	MPa	14	3.97 ± 2.39	4.69 ± 0.41	0.52
Elastic Modulus	MPa	14	38.06 ± 21.12	155.76 ± 26.59	0.01*
Failure Load	N	14	2196.19 ± 854.85	2261 ± 85.07	0.17

* indicates statistically significant differences and the significant value was 0.05

The independent two-sample t-test was chosen because the results of both experiments contained continuous and non-categorical data. The results of the t-test for stresses, elastic modulus, and failure load are, in that order, 0.52, 0.01, and 0.17. The statistical significance level was determined as 0.05. As a result, there are no statistically significant differences between compressive stresses and failure load capacities of commercial bone models and those of 3D-printed bones. On the other hand, the elastic modulus shows a significant statistical difference between composite bone models and 3D-printed bones.

4. Discussions

3DP technology still has a lot of challenges that need to be handled even if it can produce merchandise more rapidly than conventional methods. These concerns can be tackled with the help of the CJP method (Abdullah *et al.* 2019). Its capacity to spray binder and uniformly manufacture new layers over the printing area allows it to produce material faster than other printer technologies. This technique outperforms FDM technology in terms of effort and time because it doesn't need support in that the printer bed is covered in powder particles. In the study by Fatma et al. comparing FDM and CJP, it was determined that CJP required 1/3 less time than FDM on the same model (Fatma *et al.* 2021). However, this time goes up exponentially if there are more parts in the printing area. As a matter of fact, printing using CJP took 32 minutes in our study; nevertheless, if the identical samples had been printed using FDM, the printing duration may have reached as high as 380 minutes. This duration should not be underestimated in applications where rapid prototypes are at the forefront, such as preoperative planning.

Even though CJP has an edge in terms of time, its strength performance is not as desirable. Fatma et al. revealed that CJP has lower strength compared to other technologies. Similarly, Wu et al. measured an elastic modulus of 2.3 GPa according to their tests on materials produced with FDM (Wu *et al.* 2020). On the other hand, in this study, this value was calculated as 0.155 GPa, indicating that much lower strength was obtained compared to FDM. Regarding synthetic bones, on the other hand, the range of compressive strength that they achieved was 1.4 to 5.4 MPa. The mean compressive stress of artificial bone, 3.97 MPa, was pinpointed to be quite near to the Wu et al. (2020) study. Albeit not as impressive as FDM, CJP samples exhibit a mean 4.69 MPa strength advantage over artificial bones.

The elastic modulus of powder material was reported to be as high as 125 MPa in a study (Dini *et al.* 2022). According to our study, the binder dipping that was performed after the printing process was finished caused this value to escalate to a mean of 155 MPa. Furthermore, the fact that the 3DP results are much superior to artificial bones—which have an average elasticity of 38 MPa—is demonstrated. The elastic modulus of PU foam, which is formed in accordance with ISO standards, has been significantly lowered because to its comparatively greater cellular ratio as compared to solid structure. In another study, an elastic modulus of 58 MPa was obtained for Sawbone bones with a cancellous structure, which coheres the maximum value of 59 MPa we obtained in artificial bones (Zdero *et al.* 2023). In addition, elastic modulus of 3D-printed bones showed a significant difference when compared statistically with artificial bones. This is most likely because its cellular structure contains substantial quantities of artificial bone.

When it comes to cost, artificial bones are about $56, whereas 3D-printed bones cost about $15 per bone. Additionally, by using less binder in anatomical models intended for instructional uses—where strength is not a priority—cost savings can be realized. Artificial bones are being swapped with 3DP technology to diminish expenses, particularly in experiments where a large number of samples are biomechanically analyzed (Nagl *et al.* 2022). In addition, the printer device prices that this technology brings with it are another crucial factor regarding expenses. The most affordable technologies among them are SLA and FDM, whereas the most expensive machines are SLS with a laser system. CJP is somewhat more expensive than FDM even though it is less expensive than SLS. On the other hand, models with complicated geometries need to be printed with a high accuracy and resolution for these technologies to be indispensable in the healthcare industry. Although it varies across manufacturers, FDM offers axis resolutions of 0.5mm, SLA 0.2mm, and SLS 0.075mm; nevertheless, because of the tiny powder particles in CJP, this ratio can drop to 0.05mm (George *et al.* 2017). In addition, a detailed comparison of composite bones and 3DP bones is shown in Table 3.

Table 3. Comparison of composite bones and 3DP bones properties

	Composite Bones	**3DP Bones**
Comp. Stress (MPa)	1.4-5.4 (Wu *et al.* 2020) 3.97 (Our Study)	4.69 (Our Study)
Elastic Modulus (MPa)	58 (Zdero et al. 2023) 59 (Our Study)	125 (Dini et al. 2022) 155.76 (Our Study)
Cost (Per Bone, $)	56	15

3DP technology has become widespread with its affordable cost; however, it has not yet achieved the expected development in healthcare (Choonara *et al.* 2016). By eliminating a number of drawbacks between 3DP technologies, the CJP approach could be advantageous. On the other hand, artificial bones, which are widely utilized in the healthcare industry and have restricted accessibility owing to their high cost, do not provide custom-made possibilities because they follow a standardised production methodology. Thus, this technology has been initiated recently in preoperative planning because commercial composite bones are hard-to-adapt to the patient (Kadakia *et al.* 2020). In this mechanical comparison, 3D-printed and composite bones show extremely similar stress results and even a higher elastic modulus, suggesting that they might be a viable substitute for artificial bones. As a result, CJP technology does not require printing extra support. In addition, color printing may facilitate to differentiate anatomical structures easily, which may be very useful in simulation studies and medical education (Ruiz and Dhaher 2021). The CJP approach may be used in the healthcare industry to benefit greatly from the numerous advantages that this evolving and diverse technology offers. Notwithstanding the fact that 3D-printed bones indicated advantageous in this study with regard to cost, time, and durability, several limitations still need to be addressed.

Firstly, the printing area and the resolution are limited. Projet 160, used in this study, for example, has a printing volume of up to 185 x 236 x 132 mm with a printing resolution of 300 x 450 dpi. The entire femur bone of an average adult human cannot be printed using this printer. The partially printed bone parts may be a solution in this case. Thanks to rapidly developing technology, new CJP devices will have a larger build volume in the near future (Rafiee *et al.* 2020). The second drawback of this technology is the drying process following the printing. This takes about two hours or more depending on the size of the printed parts. However, since the production time is shorter than other printing methods, it compensates for this extra wait period. Finally, natural bone has anisotropic properties composed trabecular and cortical structures, though 3DP technologies can generate bone models with uniform material. This issue may be resolved by adjusting the infill ratio, one of the printing parameters, to ensure that the interior structure represents the trabecular structure. As a result of reducing this ratio, the strength of the structure can be reduced because it means less binding of powder particles that will keep up inside during printing. However, unlike other printing technologies like FDM, there must be escape holes so that powder can discharge from the enclosed area.

5. Conclusions

Rapid prototyping and high-quality models that are similar to the morphological bone structure of a patient in applications such as biomechanics-based studies and pre-operative planning have now been facilitated thanks to the innovations brought by CJP technology. However, comparing 3DP bone samples to natural bone, the mechanical properties still need to achieve the necessary standard. Therefore, this study has demonstrated that generating 3DP bone specimens instead of expensive and non-customizable composite artificial bones, which are commonly utilized, is appropriate for mechanical properties. In addition, a significant difference in elastic modulus was observed between both bone types. Nevertheless, the interior and exterior structures of natural bone cannot yet be precisely replicated by this method and 3DP models are a bit fragile. Further research is required to boost the strength using a more durable binder and to mimic the properties of natural bone's cortical and cancellous components.

Declaration of Ethical Standards

The authors declare that they comply with all ethical standards.

Credit Authorship Contribution Statement

Author-1: Conceptualization, investigation, methodology and software, validation, visualization and writing – original draft.

Author-2: Conceptualization, supervision and writing – review and editing.

Declaration of Competing Interest

The authors have no conflicts of interest to declare regarding the content of this article.

Data Availability Statement

All data generated or analyzed during this study are included in this published article.

Acknowledgement

This study was supported by Izmir Katip Celebi University Scientific Research Council Agency as project number 2023-TDR-FEBE-0005 for Samet Ciklacandir's doctoral thesis studies.

6. References

Abdullah, A. M., Mohamad, D., Din, T. N. D. T, Yahya, S., Akil, H. M., Rajion, Z. A. 2019. Fabrication of nasal prosthesis utilising an affordable 3D printer. Int J Adv Manuf Technol, **100**: 1907-1912. https://doi.org/10.1007/s00170-018-2831-y.

Al-Dulimi, Z., Wallis, M., Tan, D. K., Maniruzzaman, M., Nokhodchi, A. 2020. 3D printing technology as innovative solutions for biomedical applications. Drug Discov Today, **26**: 360-383. https://doi.org/10.1016/j.drudis.2020.11.013.

Awari, G., Thorat, C., Ambade, V., Kothari, D. P. 2021. Additive manufacturing and 3D printing technology: principles and applications. 1st ed., CRC Press, USA.

Bakhtiar, S. M., Butt, H. A., Zeb, S., Quddusi, D., M., Gul, S., Dilshad, E. 2018. 3D printing technologies and their applications in biomedical science. In: D. Barh, V. Azevedo [eds.], Omics Technologies and Bio-Engineering. Elsevier, pp. 167-189.

Beaupied, H., Lespessailles., E., Benhamou, C. L. 2007. Evaluation of macrostructural bone biomechanics. Joint Bone Spine, **74**: 233-239. https://doi.org/10.1016/j.jbspin.2007.01.019.

Blaszczyk, M., Jabbar, R., Szmyd, B., Radek, M. 2021. 3D printing of rapid, low-cost and patient-specific models of brain vasculature for use in preoperative planning in clipping of intracranial aneurysms. Journal of Clinical Medicine, **10**: 1201. https://doi.org/10.3390/jcm10061201.

Brunello, G., Sivolella, S., Meneghello, R., Ferroni, L., Gardin, C., Piattelli, A. 2016. Powder-based 3D printing for bone tissue engineering. Biotechnol Adv, **34**: 740-753. https://doi.org/10.1016/j.biotechadv.2016.03.009.

Cheng, L., Shoma Suresh, K., He, H., Rajput, R. S., Feng, Q., Ramesh, S., Ramalingam, M. 2021. 3D printing of micro-and nanoscale bone substitutes: a review on technical and translational perspectives. Int J Nanomedicine, **16**: 4289. https://doi.org/10.2147/IJN.S311001.

Choonara, Y. E., du Toit, L. C., Kumar, P., Kondiah, P. P., Pillay, V. 2016. 3D-printing and the effect on medical costs: a new era? Expert Rev Pharmacoecon Outcomes Res, **16**: 23-32. https://doi.org/10.1586/14737167.2016.1138860.

Cimerman, M., Kristan, A. 2007. Preoperative planning in pelvic and acetabular surgery: the value of advanced computerised planning modules. Injury, **38**: 442-449. https://doi.org/10.1016/j.injury.2007.01.033.

Dini, F., Ghaffari, S. A., Javadpour, J., & Rezaie, H. R. 2022. Binder jetting of hydroxyapatite/carboxymethyl chitosan/polyvinylpyrrolidone/dextrin composite: the role of polymeric adhesive and particle size distribution on printability of powders. J Mater Eng Perform, **31(7)**, 5801-5811. https://doi.org/10.1007/s11665-022-06671-1.

Du, W., Ren, X., Pei, Z., Ma, C. 2020. Ceramic binder jetting additive manufacturing: a literature review on density. J Manuf Sci Eng, **142**: 040801. https://doi.org/10.1115/1.4046248.

Dudek, P. 2013. Fdm 3D printing technology in manufacturing composite elements. Archives of metallurgy and materials, **58**: 1415-1418. https://doi.org/10.2478/amm-2013-0186.

Elfar, J., Stanbury, S., Menorca, R. M. G., Reed, J. D. 2014. Composite bone models in orthopaedic surgery research and education. J Am Acad Orthop Surg, 22: 111. https://doi.org/10.5435/JAAOS-22-02-111.

Fatma, N., Haleem, A., Javaid, M., & Khan, S. 2021. Comparison of fused deposition modeling and color jet 3D printing technologies for the printing of mathematical geometries. Journal of Industrial Integration and Management, **6**: 93-105. https://doi.org/10.1142/S2424862220500104.

Fina, F., Goyanes, A., Gaisford, S., Basit, A. W. 2017. Selective laser sintering (SLS) 3D printing of medicines. Int J Pharm, **529**: 285-293. https://doi.org/10.1016/j.ijpharm.2017.06.082.

Gardner, M. P., Chong, A. C., Pollock, A. G., Wooley, P. H. 2010. Mechanical evaluation of large-size fourth-generation composite femur and tibia models. Annals of biomedical engineering, **38**: 613-620. https://doi.org/10.1007/s10439-009-9887-7.

George, E., Liacouras, P., Rybicki, F. J., & Mitsouras, D. 2017. Measuring and establishing the accuracy and reproducibility of 3D printed medical models. Radiographics, **37(5)**: 1424-1450. https://doi.org/10.1148/rg.2017160165.

Hausmann, J. T. 2006. Sawbones in biomechanical settings-a review. Osteosynthesis and Trauma Care, **14**: 259-264. https://doi.org/10.1055/s-2006-942333.

Hochman, J. B., Kraut, J., Kazmerik, K., Unger, B. J. 2014. Generation of a 3D printed temporal bone model with internal fidelity and validation of the mechanical construct. Otolaryngol Head Neck Surg (1979), **150**: 448-454. https://doi.org/10.1177/0194599813518008.

Kadakia, R. J., Wixted, C. M., Allen, N. B., Hanselman, A. E., Adams, S. B. 2020. Clinical applications of custom 3D printed implants in complex lower extremity reconstruction. 3D Print Med, **6**: 1-6. https://doi.org/10.1186/s41205-020-00083-4.

Kim, G. B., Lee, S., Kim, H., Yang, D. H., Kim, Y. H., Kyung, Y. S., Kim, N. 2016. Three-dimensional printing: basic principles and applications in medicine and radiology. Korean J Radiol, **17**: 182-197. https://doi.org/10.3348/kjr.2016.17.2.182.

Kudelski, R., Cieslik, J., Kulpa, M., Dudek, P., Zagorski, K., Rumin, R. 2017. Comparison of cost, material and time usage in FDM and SLS 3D printing methods. 13th International conference on perspective technologies and methods in MEMS design (MEMSTECH), p. 12-14, Lviv, Ukraine.

Lee, J. Y., An, J., Chua, C. K. 2017. Fundamentals and applications of 3D printing for novel materials. Appl Mater Today, **7**: 120-133. https://doi.org/10.1016/j.apmt.2017.02.004.

Lim, K. H. A., Loo, Z. Y., Goldie, S. J., Adams, J. W., McMenamin, P. G. 2016. Use of 3D printed models in medical education: A randomized control trial comparing 3D prints versus cadaveric materials for learning external cardiac anatomy. Anat Sci Educ, **9**: 213-221. https://doi.org/10.1002/ase.1573.

Lv, X., Ye, F., Cheng, L., Fan, S., Liu, Y. 2019. Binder jetting of ceramics: Powders, binders, printing parameters, equipment, and post-treatment. Ceramics International, **45**: 12609-12624. https://doi.org/10.1016/j.ceramint.2019.04.012.

Miedzinska, D., Gieleta, R., Malek, E. 2020. Experimental study of strength properties of SLA resins under low and high strain rates. Mechanics of Materials, **141**, 103245. https://doi.org/10.1016/j.mechmat.2019.103245.

Mihcin, S., Ciklacandir, S. 2022. Towards integration of the finite element modeling technique into biomedical engineering education. Biomed Eng (Singapore), **34**: 2150054. https://doi.org/10.4015/S101623722150054X.

Nagl, K. 2021. A comparison of the biomechanical behaviour of simple artificial, composite, and 3D FDM printed human femoral bones. PhD Thesis, TU Wien, Vienna, Austria.

Nagl, K., Reisinger, A., & Pahr, D. H. 2022. The biomechanical behavior of 3D printed human femoral bones based on generic and patient-specific geometries. 3D Print Med, **8(1)**: 35. https://doi.org/10.1186/s41205-022-00162-8.

Navarro, M., Michiardi, A., Castano, O., Planell, J. A. 2008. Biomaterials in orthopaedics. J R Soc Interface, **5**: 1137-1158. https://doi.org/10.1098/rsif.2008.0151.

O'Toole III, R. V., Jaramaz, B., DiGioia III, A. M., Visnic, C. D., Reid, R. H. 1995. Biomechanics for preoperative planning and surgical simulations in orthopaedics. Comput Biol Med, **25**: 183-191. https://doi.org/10.1016/0010-4825(94)00043-P.

Rafiee, M., Farahani, R. D., Therriault, D. 2020. Multi-material 3D and 4D printing: a survey. Advanced Science, **7**: 1902307. https://doi.org/10.1002/advs.201902307.

Ruiz, O. G., Dhaher, Y. 2021. Multi-color and multi-material 3D printing of knee joint models. 3D Printing in Medicine, **7**: 1-16. https://doi.org/10.1186/s41205-021-00100-0.

Shahrubudin, N., Lee, T. C., Ramlan, R. 2019. An overview on 3D printing technology: Technological, materials, and applications. Procedia Manuf, **35**: 1286-1296. https://doi.org/10.1016/j.promfg.2019.06.089.

Tai, B. L., Kao, Y. T., Payne, N., Zheng, Y., Chen, L., Shih, A. J. 2018. 3D printed composite for simulating thermal and mechanical responses of the cortical bone in orthopaedic surgery. Med Eng Phys, **61**: 61-68. https://doi.org/10.1016/j.medengphy.2018.08.004.

Victor, S. P., Muthu, J. 2014. Polymer ceramic composite materials for orthopedic applications—relevance and need for mechanical match and bone regeneration. Journal of Mechatronics, **2**: 1-10. https://doi.org/10.1166/jom.2014.1030.

Wu, D., Spanou, A., Diez-Escudero, A., & Persson, C. 2020. 3D-printed PLA/HA composite structures as synthetic trabecular bone: A feasibility study using fused deposition modeling. J Mech Behav Biomed Mater, **103**: 103608. https://doi.org/10.1016/j.jmbbm.2019.103608.

Wu, G., Zhou, B., Bi, Y., Zhao, Y. 2008. Selective laser sintering technology for customized fabrication of facial prostheses. The Journal of prosthetic dentistry, **100**: 56-60. https://doi.org/10.1016/S0022-3913(08)60138-9.

Xu, N., Ye, X., Wei, D., Zhong, J., Chen, Y., Xu, G., He, D. 2014. 3D artificial bones for bone repair prepared by computed tomography-guided fused deposition modeling for bone repair. ACS Appl Mater Interfaces, **6**: 14952-14963. https://doi.org/10.1021/am502716t.

Zdero, R., Brzozowski, P., & Schemitsch, E. H. 2023. Biomechanical properties of artificial bones made by Sawbones: A review. Med Eng Phys, 104017. https://doi.org/10.1016/j.medengphy.2023.104017.

Zhang, J., Allardyce, B. J., Rajkhowa, R., Wang, X., Liu, X. 2021. 3D printing of silk powder by binder jetting technique. Addit Manuf, **38**, 101820. https://doi.org/10.1016/j.addma.2020.101820.

Ziaee, M., Crane, N. B. 2019. Binder jetting: A review of process, materials, and methods. Addit Manuf, **28**: 781–801. https://doi.org/10.1016/j.addma.2019.05.031.